The Transformative Tricopter

1st Jasper Lee
Department of Mechanical Engineering
Massachusetts Institute of Technology
Cambridge, MA, USA
repsaj17@mit.edu

2nd Jean-Marc Ingargiola
SBI Biorobotique
Aix-Marseille Université
Marseille, France
jean-marc.ingargiola@univ-amu.fr

3rd Stéphane Viollet
SBI Biorobotique
Aix-Marseille Université
Marseille, France
stephane.viollet@univ-amu.fr

***Abstract*—Bio-inspired design has gained popularity in robotics for offering structural transformation and adaptability, suitable for changing environmental conditions. While morphing mechanisms have been explored for unmanned aerial vehicles (UAVs), there is a paucity of attention to tricopters—a unique UAV configuration known for its agility, stability, and energy efficiency. This paper presents a novel transforming tricopter design, detailing its mechanical architecture, flight dynamics, autopilot, software implementation and potential applications. Key contributions include analysis of the transformation mechanism, system dynamics, and proposed directions for future development.**

I. Introduction

Whether it be package deliveries, disaster relief, agriculture, or military tactical use, drones will continue to fill its role as a cornerstone for technological development. With its vast amount of applications, drones lack the ability to transform, and to "morph", changing size, shape, and agility presented with various environmental conditions, as seen in birds. Not only are these aerial creatures able to vary their aerodynamics at will with their foldable wings and overlappable feathers, they are able to conduct rapid adaptation and optimization suitable for hunting, fleeing and energy efficiency [1]. By integrating characteristics of wildlife, drones would be able to navigate narrow openings needed for search and rescue, rapidly adapt to atmospheric conditions, optimize energy consumption, and minimize radio wave reflections for military stealth to name a few examples. Although there exists research on this topic with transformative drones [2], [6], [10], tricopters, unlike other multirotor designs, offer unparalleled speed and agility; therefore, this transformative tricopter takes the leap in bringing our rigid aerial vehicles one step closer to the functionalities of our flying friends, all the while retaining the strength and robust qualities of a drone.

II. Related Work

Although similar shape-shifting drones have been developed [2], [3], [5], [10], the degree of their transformations is often limited to one arm actuated movements, limiting their expansion, and therefore range of adaptation. For example, in [2], the fully expanded and contracted states of the 'Foldable Drone' are targeted for object inspection and crevice navigation and are not suitable for extreme changes in environmental conditions, where rapid change in drone dynamics is necessary while maintaining stability. However, the sliding arm quadcopter [3] changes its shape through arm extensions, consequently moving the center of mass; however this design too, doesn't change its rotational inertia significantly, as seen from its minimal pitch and yaw rotations. As for Morpho-Copter [5], the drone is only able to change the angle of its arms, and its four servo motors makes it prone to failures, according to the authors. Given the complexity of current morphing drones, with numerous servo motors, the drones do not achieve large increases in width, which is why this transformative tri-copter utilizes truss-like mechanisms to simplify the servo motor complexity while maximizing adaptation and stability with expansion.

Fig. 1. Tricopter expansion evolution.

III. Mechanical Design

In light of transformative mechanisms often requiring multiple components—thus adding weight and complexity—the 2D-truss approach was taken, rendering all twelve tri-copter arms simple two-force members that were thin, lightweight, and straightforward to fabricate. To lubricate rotational joints, 2 mm Teflon spacers proved to be a light and effective solution, in contrast to the weight of ball bearings.

Given the need for planar movement and weight optimization, a coaxial motor was implemented as opposed to the conventional tilt servo, where the counterrotating propellers (one CW, one CCW) produce equal and opposite reaction torques on the airframe, resulting in a net yaw torque of approximately zero. Controlled by a servo motor, the rotor (small triangular base) actuates the expansion mechanism through rotational movement, as seen in the progression from

Fig. 3 to Fig. 4. Cross-sectional area of the tri-copter is plotted against the rotation angle γ. This rotational actuation about the z-axis maintains stability in roll, pitch, and yaw due to the conservation of angular momentum, while changing the rotational inertia to allow for agility and speed.

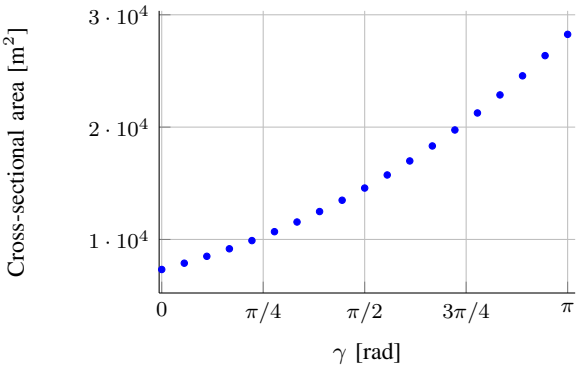

Fig. 2. Graph of Top-Down Cross-sectional Area vs. Deploy Angle (γ), proportional to kx^2, where $k \in \mathbb{R}$.

Through serial radio communication, the `Elev D/R` toggle allows the drone to expand and contract mid-air (dynamics to be discussed in *Dynamic Modeling Section*). At an initial top-down cross-sectional area of 7,317.352 mm^2 mapped by central motor-mounted points, the tri-copter is capable of expanding to more than triple its original area at 23,482.812 mm^2, as shown in Fig. 3 and Fig. 4. For the principal-axis rotational inertia, the tri-copter starts at $L_{xx} = 7.1 \times 10^{-4}\,\text{kg}\,\text{m}^2$, $L_{yy} = 7.6 \times 10^{-4}\,\text{kg}\,\text{m}^2$, $L_{zz} = 9.9 \times 10^{-4}\,\text{kg}\,\text{m}^2$, and morphs to $L_{xx} = 1.7 \times 10^{-3}\,\text{kg}\,\text{m}^2$, $L_{yy} = 1.6 \times 10^{-3}\,\text{kg}\,\text{m}^2$, $L_{zz} = 2.9 \times 10^{-3}\,\text{kg}\,\text{m}^2$. This not only creates significant advantages in stability, but also enables the UAV to alter its dynamics midair in response to environmental conditions, such as air drag. Finally, a custom triangular PCB board is mounted on the drone to provide compact yet easily accessible integration of electronics.

IV. Dynamic Modeling

In this section, we develop the equations of motion (EOMs) for the tri-copter using Lagrangian mechanics, an energy-based formulation. The generalized coordinates (GCs) defined with respect to inertial frame $\mathcal{I}$ are:

$$\mathbf{q} = \begin{bmatrix} \mathbf{q}_T \\ \mathbf{q}_R \end{bmatrix} \quad \text{where} \quad \mathbf{q}_T = \begin{bmatrix} x \\ y \\ z \end{bmatrix}, \quad \mathbf{q}_R = \begin{bmatrix} \psi \\ \theta \\ \phi \end{bmatrix} \tag{1}$$

A. Assumptions and Moment of Inertia Formulation

In this analysis, we assume the tri-copter is in hovering state, resulting in negligible drag forces since $F_{\text{drag}} \propto v^2$. Furthermore, gyroscopic effects are considered insignificant due to minimal yaw rates and low servomotor rotation speed $\dot{\gamma}$. As the servo motor rotates clockwise, the drone deploys, both increasing its moment of inertia (MoI) and generating body yaw movement counterclockwise (conservation of angular momentum). Thus, the MoI $I(\gamma, t)$ depends on γ and time.

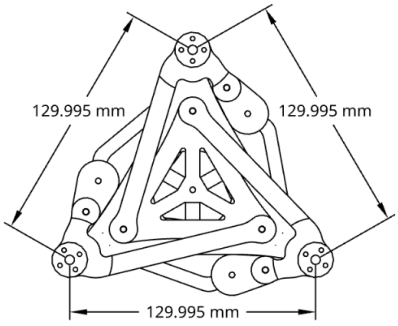

Fig. 3. Tricopter in its most compact state at a rotor rotation of 0 radians.

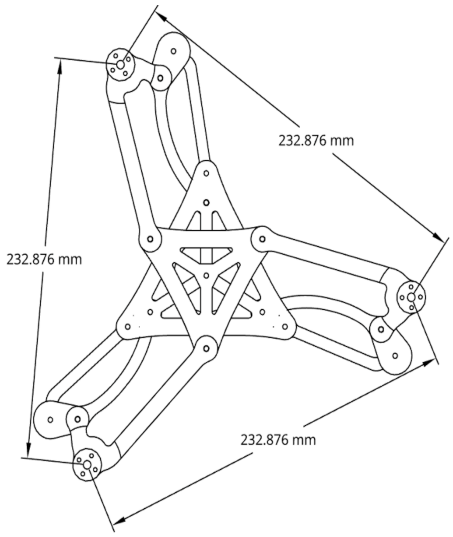

Fig. 4. Tricopter in its fully deployed state at a rotor rotation of π radians.

B. The Lagrangian

The Lagrangian is defined as:

$$\mathcal{L}(q_i, \dot{q}_i, t) = T(q_i, \dot{q}_i, t) - V(q_i, t) \tag{2}$$

where T is the kinetic energy and V is the potential energy. When internal actuation of γ induces global angular motion ψ, the total kinetic energy includes both the global yaw and the relative rotation of the internal mechanism, which we call a 'rotor.' However, given the negligible weight and rotation speed of the rotor, we absorb this term into that of the entire drone. M denotes the mass of the entire drone.

$$\mathcal{L} = \frac{1}{2} \dot{q_T^T} M \dot{q_T} + \frac{1}{2} \dot{q_R^T} \mathbb{J}_\text{b}(\gamma, t) \dot{q_R} - Mgz \tag{3}$$

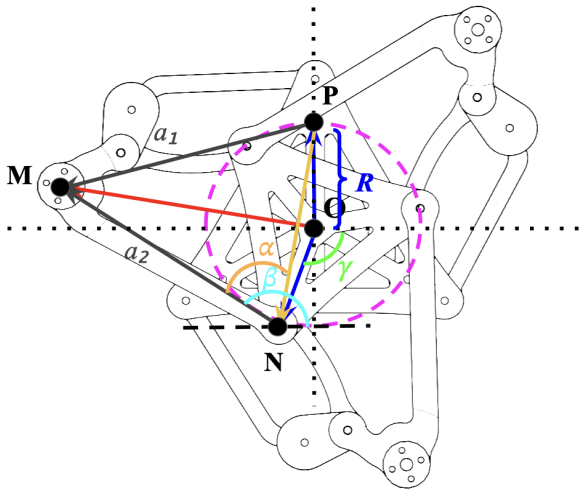

Fig. 5. Diagram showing the motor's position vector dependent on rotor rotation γ and subsequent angles α and β.

C. Generalized Forces

To account for and symbolically describe the forces exerted on the system, we introduce generalized forces (GFs) for each GC.

$$\mathbf{Q} = \begin{bmatrix} \mathbf{Q}_T \\ \mathbf{Q}_R \end{bmatrix} \quad \text{where} \quad \mathbf{Q}_T = \begin{bmatrix} Q_x \\ Q_y \\ Q_z \end{bmatrix}, \quad \mathbf{Q}_R = \begin{bmatrix} Q_\psi \\ Q_\theta \\ Q_\phi \end{bmatrix} \tag{4}$$

To calculate the GFs, we find the position vector of each motor, $\vec{r_{\text{OM}}}$ (see the derivation in Appendix):

$$\vec{r}_{\text{ON}} = R \begin{bmatrix} \cos\gamma \\ -\sin\gamma \end{bmatrix} \tag{5}$$

$$\vec{r}_{\text{NM}} = a_1 \begin{bmatrix} \cos\beta \\ \sin\beta \end{bmatrix}, \text{ where } \beta(\gamma) = \frac{3\pi}{4} - \frac{\gamma}{2} + \alpha(\gamma) \tag{6}$$

$$\vec{r}_{\text{OM}} = \vec{r}_{\text{ON}} + \vec{r}_{\text{NM}} \tag{7}$$

Let $\vec{r}_n = \begin{bmatrix} \cos(\frac{2\pi}{3}n) & \sin(\frac{2\pi}{3}n) \\ -\sin(\frac{2\pi}{3}n) & \cos(\frac{2\pi}{3}n) \end{bmatrix} \vec{r}_{\text{OM}}$ denoting the position of the n-th motor, each separated by $\frac{2\pi}{3}$ radians, where n = 1, 2, 3. We find $\mathbf{Q}_T = \left(\mathbf{R} \cdot \vec{F}_{\text{body}} + \vec{F}_g\right)$.

$$\vec{F}_{\text{body}} = \begin{bmatrix} 0 \\ 0 \\ -(T_1+T_2+T_3) \end{bmatrix}, \quad \vec{F}_{\text{g}} = \begin{bmatrix} 0 \\ 0 \\ -Mg \end{bmatrix} \tag{8}$$

$$\mathbf{R} = \begin{bmatrix} c_\theta c_\psi & c_\theta s_\psi & -s_\theta \\ s_\phi s_\theta c_\psi - c_\phi s_\psi & s_\phi s_\theta s_\psi + c_\phi c_\psi & s_\phi c_\theta \\ c_\phi s_\theta c_\psi + s_\phi s_\psi & c_\phi s_\theta s_\psi - s_\phi c_\psi & c_\phi c_\theta \end{bmatrix} \tag{9}$$

On the other hand, $\mathbf{Q}_R = \vec{\tau}$, where $\delta = arctan(\frac{\vec{r_n}\cdot\hat{j}}{\vec{r_n}\cdot\hat{i}})$.

$$\vec{\tau} = \begin{bmatrix} \sum_{n=1}^{3} C_Q \rho ||\vec{r}_n||^5 \omega_n^2 \\ \sum_{n=1}^{3} (\vec{r_n} \cdot \hat{i}) \times T_n \\ \sum_{n=1}^{3} (\vec{r_n} \cdot \hat{j}) \times T_n \end{bmatrix} \tag{10}$$

Our Euler-Lagrangian becomes:

$$\frac{d}{dt}\left(\frac{\partial L}{\partial \dot{q}_i}\right) - \frac{\partial L}{\partial q_i} = Q \tag{11}$$

and we obtain the EOMs:

$$M\ddot{q_T} + \begin{bmatrix} 0 \\ 0 \\ Mg \end{bmatrix} = Q_T \tag{12}$$

$$\mathbb{J}\ddot{q_R} + \dot{\mathbb{J}}_b \dot{q_R} - \frac{1}{2}\frac{\partial}{\partial q_R}(\dot{q_R}\mathbb{J}_b\dot{q}) = Q_R \tag{13}$$

Factoring out $\dot{q_R}$, we find the Coriolis terms containing the gyroscopic and centrifugal terms:

$$C(q_R, \dot{q_R}) = [\dot{\mathbb{J}}_b - \frac{1}{2}\frac{\partial}{\partial q_R}(\dot{q_R^T}\mathbb{J}_b)]\dot{q_R} \tag{14}$$

Simplifying (12) and (13), our EOMs become:

$$M\ddot{q_T} = (T_1+T_2+T_3)\begin{bmatrix} -sin(\theta) \\ cos(\theta)sin(\phi) \\ cos(\theta)cos(\phi) \end{bmatrix} + \begin{bmatrix} 0 \\ 0 \\ -Mg \end{bmatrix} \tag{15}$$

$$\mathbb{J}\ddot{q_T} = C(q_R, \dot{q_R}) + \tau \tag{16}$$

V. Autopilot Software Implementation

A simple command loop based on DRhem VTOL was implemented for this tri-copter. The controller begins by passing in raw IMU gyro and accelerometer values for each axis into the Madgwick filter, which then calculates a prediction step and gradient-descent-based correction step to arrive at an attitude estimation; these values are converted into angles. Next, the pilot's RC commands are converted into values $\in [0,1]$ or $[-1,1]$ depending on the Euler angle and sent to the PID Control for error estimation based on the IMU angle calculation. This returns roll, pitch and yaw PID values between 0 and 1 that represent 1-D stabilized signals. Finally, the mixer function fuses these signals and sends the commands to the motors. With this flight controller, we are able to establish resilience in roll, pitch and yaw [Fig 6], as the drone lifts off into hover state [Fig-7].

VI. Conclusion

We show that this transforming tri-copter drone can adapt effectively in size, changing its cross-sectional area by a factor of three, and successfully maintain resilience in roll, pitch, and yaw during the flight tests conducted. Future applications include package deliveries, disaster relief, agriculture, or military tactical advantages.

Acknowledgment

The authors would like to acknowledge the sponsorship and support by the SBI Biorobotique Laboratory at the Aix-Marseille University and the Massachusetts Institute of Technology under the France MISTI Program.

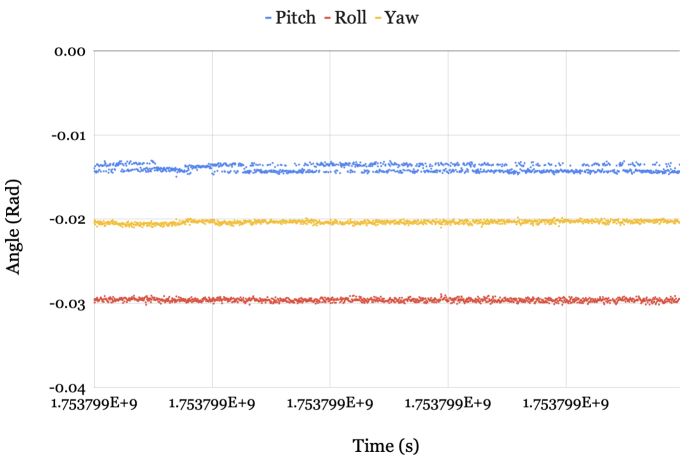

Fig. 6. Graph showing pitch, roll and yaw with respect to time.

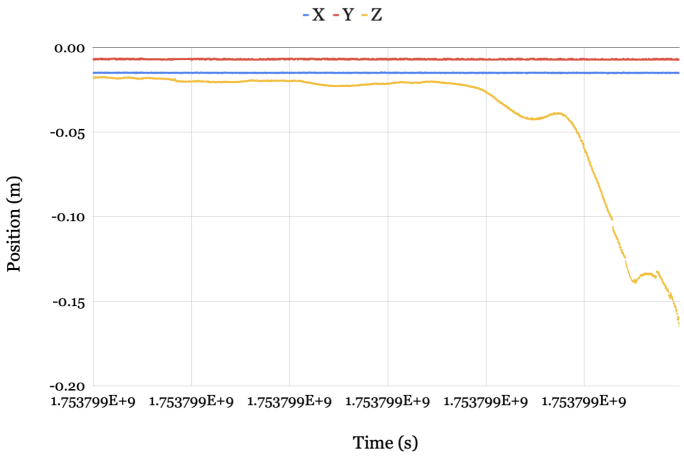

Fig. 7. Graph showing position in x, y, z with respect to time, with the z axis is pointing down.

Appendix: Full Derivation

Given the controlled rotor rotation angle γ, we solve for angles $\alpha(\gamma)$ and $\beta(\gamma)$ as functions of γ.Using the law of cosines and trigonometric manipulation, we find

$$\alpha = \arccos\left(\frac{\|\vec{a}_1\|^2 + \|\vec{r}_{ON} - \vec{r}_{OP}\|^2 - \|\vec{a}_2\|^2}{2\,\|\vec{a}_1\|\,\|\vec{r}_{ON} - \vec{r}_{OP}\|}\right) \tag{17}$$

$$\beta(\gamma) = (\pi - \gamma) + (\frac{\gamma}{2} - \frac{\pi}{4}) + \alpha(\gamma) \tag{18}$$

where

$$\vec{r}_{\text{OP}} = \begin{bmatrix} 0 \\ 1 \end{bmatrix} \tag{19}$$

As seen in Fig. 5, we simply swap in the dynamic variables to find the respective positions of the motors.

References

[1] S. Mintchev and D. Floreano, "Adaptive Morphology: A Design Principle for Multimodal and Multifunctional Robots," in IEEE Robotics & Automation Magazine, vol. 23, no. 3, pp. 42-54, Sept 2016.

[2] D. Falanga, K. Kleber, S. Mintchev, D. Floreano and D. Scaramuzza, "The Foldable Drone: A Morphing Quadrotor That Can Squeeze and Fly," in IEEE Robotics and Automation Letters, vol. 4, no. 2, pp. 209-216, April 2019.

[3] R. Kumar, A. Deshpande, J. Wells and M. Kumar. (2020). "Flight Control of Sliding Arm Quadcopter with Dynamic Structural Parameters," in 2020 IEEE/RSJ International Conference on Intelligent Robots and Systems (IROS), October 2020.

[4] V. Riviere, A. Manecy, and S. Viollet, "Agile robotic fliers: A morphing-based approach," Soft robotics, pp. 541–553, 2018

[5] H. Modi, H. Su, X. Liang, M. Zheng, "MorphoCopter: Design, Modeling, and Control of a New Transformable Quad-Bi Copter", 2025 IEEE International Conference on Robotics and Automation (ICRA), June 2025

[6] N. Bucki and M. W. Mueller, "Design and control of a passively morphing quadcopter," in 2019 International Conference on Robotics and Automation (ICRA). IEEE, 2019, pp. 9116–9122.

[7] J. Delmerico, S. Mintchev, A. Giusti, B. Gromov, K. Melo, T. Horvat, C. Cadena, M. Hutter, A. Ijspeert, D. Floreano et al., "The current state and future outlook of rescue robotics," Journal of Field Robotics, vol. 36, no. 7, pp. 1171–1191, 2019.

[8] G. Nandakumar, A. Srinivasan, and A. Thondiyath, "Theoretical and experimental investigations on the effect of overlap and offset on the design of a novel quadrotor configuration, voops," Journal of Intelligent & Robotic Systems, pp. 615–628, 2018.

[9] P. Pounds, R. Mahony, J. Gresham, P. Corke, and J. M. Roberts, "Towards dynamically-favourable quad-rotor aerial robots," in Proceedings of the 2004 Australasian Conference on Robotics & Automation. Australian Robotics & Automation Association, 2004.

[10] M. Zhao, T. Anzai, F. Shi, X. Chen, K. Okada, and M. Inaba, "Design, modeling, and control of an aerial robot dragon: A dual-rotor- embedded multilink robot with the ability of multi-degree-of-freedom aerial transformation," IEEE Robotics and Automation Letters, pp. 1176–1183, 2018.

[11] J. Lane, N. Hyun, "Graph-Based Dynamics and Network Control of a Single Articulated Robotic System", 2025 American Control Conference (ACC), pp.2003-2010, 2025.

[12] M. Zhao, "Aerial Grasping by Multi-Limbed Flying Robot SPIDAR Based on Vectored Thrust Control", 2025 IEEE International Conference on Robotics and Automation (ICRA), pp.5202-5208, 2025.

[13] S.Hameed, A. Jie, N. Imanberdiyev, E. Camci, W. Yau, M. Feroskhan, "Dragonfly Drone: A Novel Tilt-Rotor Aerial Platform with Body-Morphing Capability", 2025 IEEE International Conference on Robotics and Automation (ICRA), pp.8642-8648, 2025.

[14] Q. Pan, X. Lu, W. Yuan, F. Li, "MRBicopter: Modular Reconfigurable Transverse Tilt-Rotor Bicopter System", 2024 14th International Conference on Information Science and Technology (ICIST), pp.254-260, 2024.

[15] N. Mahadi, R. Yoshimura, J. Woo, Y. Ohyama, "Development of a Modular Structured Drone System to Enhance Robotic Functionality", 2024 Joint 13th International Conference on Soft Computing and Intelligent Systems and 25th International Symposium on Advanced Intelligent Systems (SCIS&ISIS), pp.1-6, 2024.

[16] A. Kumutham, D. Pratihar, A. Deb, "Impact of CoM Placement on Quadcopter's Performance and Controller Development", 2024 36th Conference of Open Innovations Association (FRUCT), pp.331-336, 2024.

[17] J. C. Gomez and E. Garcia, "Morphing unmanned aerial vehicles," Smart Mater. Struct., vol. 20, no. 10, p. 103001, 2011.

[18] W. M. Shen, M. Krivokon, H. Chiu, J. Everist, M. Rubenstein, and J. Venkatesh, "Multimode locomotion via SuperBot reconfigurable robots," Autonomous Robots, vol. 20, no. 2, pp. 165–177, 2006.

[19] A. Fabris, K. Kleber, D. Falanga and D. Scaramuzza, "Geometry-aware Compensation Scheme for Morphing Drones," 2021 IEEE International Conference on Robotics and Automation (ICRA), Xi'an, China, 2021.

[20] Y. Bai and S. Gururajan, "Evaluation of a baseline controller for autonomous "figure-8" flights of a morphing geometry quadcopter: Flight performance," Drones, p. 70, 2019.